EUROPEAN ORGANIZATION FOR NUCLEAR RESEARCH

CLARIFICATION LETTER

to the ISOLDE and Neutron Time-of-Flight Committee

INTC-P-666: Study of the Coulomb barrier scattering of ^{10}C with heavy targets

I. Martel and N. Keeley,
on behalf of the INTC-P-666 Collaboration

*INTC Report included in ANNEX 1, pg. 12.

1. Preliminary remarks

The aim of the proposed experiment is to measure for the first time the cross sections of the elastic, inelastic (^{10}C*), and transfer reaction channels (^{11}C) of the scattering system ^{10}C+^{208}Pb around the Coulomb barrier (Eb~ 60 MeV Lab), delivering the total cross sections and their angular distributions. We would like to remark that although elastic data exist at 66 MeV from the work of Linares et al., PRC 103, 044613 (2021), there are no data on the relevant reaction channels. Therefore, the complete data set to be obtained in the proposal IS-666, which includes elastic, inelastic and transfer, does not exist and is completely new. These new data are necessary to determine the contribution of these reaction processes to the total reaction cross section and learn about the dynamics of the system, but also to probe theoretical models and calculations.

Some questions that we will answer, just from the new data (no theory required) are the following: To what extend is the reaction dynamics dominated by ^{11}C transfer and ^{10}C excitation? How does the strong Coulomb field of the ^{208}Pb target affect the reaction dynamics, as compared to the ^{58}Ni target (Guimarães, et al., PRC100, 034603 (2019)) where the Coulomb field is much weaker? Is there a Coulomb rainbow in the ^{10}C+^{208}Pb system at Coulomb barrier energies? One should note that the ^{12}C+^{208}Pb scattering system measured by S. Santra et al., PRC 64 (2001)024602 over a wide range of energies around the Coulomb barrier (see Fig. 1) shows a Coulomb rainbow, as does the scattering of the exotic ^{10}C by ^{58}Ni measured by Guimarães, et al. PRC100, 034603 (2019) at energies close to the Coulomb barrier. However, the Coulomb rainbow is absent in the data measured by Linares et al. using a ^{208}Pb target. What makes the ^{208}Pb target so special? Our collaboration recently measured the ^{17}Ne+^{208}Pb system around the Coulomb barrier (J. Diaz et al., PLB 843 (2023) 138007) and found the absence of a Coulomb rainbow. Is it then that the Coulomb barrier dynamics of ^{10}C is like that of ^{17}Ne? The answers to these questions will follow directly from the new data to be obtained by IS-666 at ISOLDE; they do not depend on the theory.

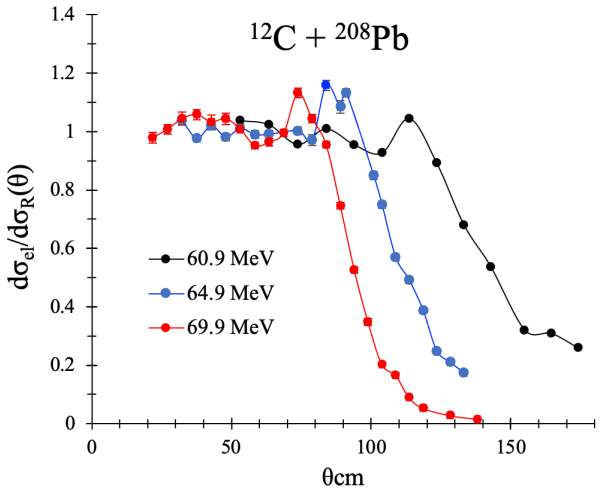

Figure 1. *A selection of elastic cross section data for the scattering system ^{12}C + ^{208}Pb at collision energies E= 60.9 MeV, 64.9 MeV, 69.9 MeV, just around the Coulomb barrier. The data was taken from S. Santra et al., PRC 64 (2001) 024602. The lines shown are just to guide the eye. See text for discussion.*

The new data are also very important to tune the theoretical calculations, which can go beyond the more standard 3- or 4- body approaches, and perhaps will require a complete 5- body description as pointed out by the referees and Linares et al., but still not developed by theoreticians. On the theoretical side we plan to study coupling effects using Optical Model (OM), Coupled Channels (CC), Continuum Discretised CC calculations (CDCC), and Coupled Reaction Channel Calculations (CRC) in line with the analysis performed by Guimarães, et al. Our team has long experience with these calculations. The reaction cross sections will be obtained using OM calculations reproducing the angular distribution of the elastic channel, which may be compared with those obtained for other halo systems. CC and CDCC calculations will allow us to investigate the coupling between elastic scattering, inelastic scattering, and the continuum, and the CRC calculations the coupling to the transfer channel. Altogether our study will provide for the first time a complete picture of the dynamics of ^{10}C at Coulomb barrier energies, for the scattering with a very high-Z target (^{208}Pb) and thus dominated by a strong Coulomb field. Some questions that will be answered are the following: Is coupling to the continuum actually important, given the relatively large threshold energies (in excess of 3 MeV)? How do the elastic, inelastic excitation, and transfer couple together? How are the coupling effects affected by the very strong Coulomb field, as compared to the lighter ^{58}Ni target used by Guimarães, et al.? How does it compare to the Coulomb barrier scattering of other proton rich systems like ^{8}B or ^{17}Ne? In addition to this, the data will be used to trigger more complex theoretical studies based on 4- (M. Rodríguez-Gallardo and Jesús Casal, EPJ Web of Conferences 252, 04004 (2021)) and 5-body models.

2. Answer to the questions

- ***The proponents should prove that their devices can distinguish between both channels. They should also say whether they can disentangle the excitation of the Pb target from that of ^{10}C.***

We note that according to the data for the $^{12}C+^{208}Pb$ scattering system measured by S. Santra et al., PRC 64 (2001) 024602 at 69.9 MeV Lab (very close to the 70 MeV scattering energy of our proposal) the contribution of $^{208}Pb^*$ inelastic should be very small $\sim<$ 4 mb/sr along the full angular range. Nevertheless, the $^{208}Pb^*$ inelastic process has been included in the simulations of the detector system.

For simulating the detector system, the codes MATHEMATICA and LISE++ were used. As the target is tilted by 45°, and the pixels are not perpendicular to the reaction point, the geometry of GLORIA cannot be directly implemented in LISE++. Therefore, MATHEMATICA was used to implement the 3D geometry of the GLORIA array, delivering for each observation angle (pixel) the target and detector thicknesses, the angular region covered, and the corresponding solid angles. These data were then supplied to LISE++ to carry out the Montecarlo simulations. The geometry of the detector setup is discussed in *Section 1*, and the physics simulations in *Section 2*.

Section 1. Detector geometry

In this experimental setup each of the particle detectors (telescopes) A, B, C, D, E, F of the GLORIA system (G. Marquínez-Durán et al., NIMA 755, 69 (2014)) is composed of two superimposed silicon layers of identical size 50 x 50 mm, namely *DE* and *E* respectively, which are separated by only ~ 2 mm (PCB frame). Total energy *Et* of each event is obtained by adding the corresponding detector signals, $Et = DE + E$. The *DE* detector is ~ 40 μm thick (10% variation along the surface) and is segmented in 16 (vertical) x 16 (horizontal) strips of 3.125 mm width, allowing for 256 position pixels (XY). The *E* detector is just a plain silicon PAD of ~ 500 μm thickness. These detectors are provided by Micron Semiconductors Ltd, models W1-DS (for *DE*) and MSX25 (for *E*). The detectors A, B, C, D, E, F are placed in a very close geometry where the centre of each *DE* is at 35 mm from the reaction point (target), and the scattering angle is determined by the relative position of each pixel.

The 3D geometry of the detector array is shown in the top-left panel of Fig. 2, and the intrinsic coordinate system (X, Y) locating each detector pixel is shown in the top-right panel (the target is

always facing the detector). Selected pixels of detectors A (1, 1), E (8, 8), D (1, 7) are shown in the central panel. The angular coverage of detectors ABCD is about 50°, and 90° for EF. For a given pixel, the angular coverage is ~ 4.5° if located at the central region of the detector (e.g., pixel 1,1) and about ~ 2° at the corners (e.g., pixel 8,8). As expected, there are angular regions covered by detectors A,B and C,D that overlaps with E,F. A summary of the relevant geometrical features is given in Table 1.

The target geometry is shown in the bottom panel of Fig. 2. The reaction is assumed to occur at the centre of the target (thickness T=1.1 μm) tilted 45° lab. For the simulations one must consider the corresponding beam energy loss δE_{tgt}, energy and angular straggling for distance $T_{1/2,\,eff}$ = T Cos (45°)/2 = 0.78 μm. After the scattering process, elastic and reaction fragments must travel a distance T_{scatt} (θ_{scatt}, Φ_{scatt}) through the target material before reaching a given detector pixel characterised by the scattering angle θ_{scatt} , and polar angle Φ_{scatt}. The reaction fragments will punch through the detector pixel, losing an energy *DE* (θ_{scatt}, Φ_{scatt}), which depends on the effective silicon pixel thickness T_{DE}($\theta_{scatt,}$ Φ_{scatt}). A nominal thickness of 40 μm was used for DE. Finally, the fragments will be stopped in the thick *E* detector, which is not position sensitive, with a nominal thickness of 500 μm. The total energy of the event can be reconstructed as $E_T(\theta_{scatt}, \Phi_{scatt}) = DE(\theta_{scatt}, \Phi_{scatt}) + E(\theta_{scatt}, \Phi_{scatt}) + \delta E_{tgt}$. The values of $T_{scatt}(\theta_{scatt}, \Phi_{scatt})$, $T_{DE}(\theta_{scatt}, \Phi_{scatt})$ were obtained from the geometrical model implemented in Mathematica. The energy losses *DE* (θ_{scatt}, Φ_{scatt}), *E* (θ_{scatt}, Φ_{scatt}) and δE_{tgt}, plus the corresponding energy and angular straggling, were calculated using LISE++.

To extract the cross sections, events of pixels for angles within 5° angular difference can be added together. A selection of θ_{scatt} angular regions of this experiment for each detector is shown in Fig. 3: 60°-65° (green), 80°- 85° (pink), 115°- 120° (light blue). The number of pixels included in the present study is also given in the figure (the excluded pixels due to target shadow effects are discussed below).

It is also possible directly to add the spectrum of the pixels corresponding to a given scattering angle, a generally extended practice that can significantly reduce the time needed to complete the data analysis process. However, to avoid the degradation of energy and mass resolution, the energy distributions of *DE* and *Et* must be corrected for various effects. The kinetic energy spread produced by the angular window covered by each pixel (~ 4.5°) is below ~ 50 keV and the overall effect is small. The main contributions to the energy/mass resolution of the sum spectrum are the thicknesses of the target and *DE* detector pixels, $T_{scatt}(\theta_{scatt}, \Phi_{scatt})$ and $T_{DE}(\theta_{scatt}, \Phi_{scatt})$ respectively, which depend on the polar angle Φ. Additional effects can arise from gain shifts in the preamps and shapers (electronics chain). These effects can be corrected by measuring the elastic channel of a ^{12}C stable beam at the same collision energy (70 MeV). The stable beam will also provide an additional reference for the normalisation of the cross sections, a measurement of pixel solid angles, and an additional point (to the ^{10}C elastic peak) for the energy calibration; it will also serve to fine-tune the dynamical range, the overall electronics and DAC system. We have requested a shift (8 hours) of ^{12}C at 70 MeV for this experiment. Further details about the setup and data analysis of the GLORIA detector array can be found in the PhD of G. Marquínez Durán, University of Huelva, 2015 [https://rabida.uhu.es/dspace/handle/10272/12397].

The detectors E, F of the proposed detector setup (above/below the tilted target) will provide the relevant cross sections in the angular range 46° - 134° (Table 1). The shadow region of the target lies over the diagonal of detectors A, B, C, D, the corresponding pixels shown in Fig. 3 in dark blue (T_{eff} > 3.5 um) and red (θ ~ 90°, T_{eff} ~infinity). For the former, the combined action of target energy loss and straggling will preclude the separation of the inelastic channels, (although elastic and transfer channels might still be extracted); and for the latter, elastic and reaction fragments are just stopped in the target. There is a total of 46 "non-valid" pixels of the 256 available for each detector A, B, C or D, which amounts to about ~ 20% surface loss. None of these pixels have been considered in the present study.

In the standard GLORIA configuration, the target detector-centre distance is 60 mm; all the pixels in the A, B, C, D detectors are "valid", and the single-pixel angular resolution is ~3°. In the proposed configuration, the target detector-centre distance is 35 mm, the angular resolution is ~ 5°, but the total solid angle increases by a factor ~ $(60/35)^2$ ~ 300%. By subtracting the contribution of the "non-valid" pixels there is a net gain of ~ 280% in detector efficiency. Summarising, the proposed configuration allows us to reduce the beam time request by a factor ~3 to achieve the required statistics, a very important feature for radioactive beam experiments.

Section 2. Montecarlo simulations

As described in the previous section, the reaction is assumed to occur at the centre of the target tilted 45°. The characteristics of the reaction fragments at this point were obtained using the calculators (Physics, Kinematics). The Montecarlo simulation was carried out, for each selected detector pixel, using a beam of the corresponding energy, and the corresponding values of target thickness and DE thickness obtained from Mathematica. A summary is given below:

1. The Kinematics Calculator toolkit was used to obtain the energy loss δE_{tgt} and outgoing energies E_{out} of relevant reaction channels using a ^{10}C beam at E= 70 MeV (lab) and target thickness $T_{eff,1/2}$= 0,78 um. The corresponding energy and angular straggling of the ejectiles were obtained from the Physics Calculator. The kinematics spread through the pixel window of 5° was obtained using the Kinematics Calculator. The angular and energy spread calculated at the target centre were much smaller than those of the HIE-ISOLDE beam itself, so these were taken for the simulations.

2. The input beam consisted of ions of ^{10}C (or ^{11}C) at the corresponding E_{out} values. A global energy spread (FWHM) of 300 keV, a spot size of 3 x 3 mm and a divergence parameter of 10° (twice the angular spread on the pixel window) was used for the simulations.

4. The detector configuration was a silicon telescope of two stages DE + E. Target and DE detector thicknesses were taken as $T_{scatt}(\theta_{scatt}, \Phi_{scatt})$ and $T_{DE}(\theta_{scatt}, \Phi_{scatt})$ as obtained from Mathematica, whereas the thickness of E was kept constant at 500 μm.

5. The simulations were carried out for the reaction channels ^{10}C elastic, ^{10}C*(3.35 MeV), ^{208}Pb*(2.6 MeV), and transfer to ^{11}C (gs, Q= +5.75 MeV). The scattering angles selected (60°, 80°, 115°) correspond to the position of the maxima of the angular distribution of the elastic cross section (Coulomb rainbow), inelastic ^{10}C* and neutron transfer to ^{11}C. A constant value of 4 mb/sr was assumed for the cross section of ^{208}Pb*.

6. The number of events in the spectra correspond to the total expected statistics for the given angles, and the number of events of each channel are distributed according to the cross sections.

7. The pixels simulated have been selected using the following criteria. Pixel FG (5,5) corresponds to θ_{scatt} = 60°-65° and is placed at the centre of the detector (marked with "b" in the green area shown in the picture of Fig. 3 centre panel). This provides a typical particle identification and corresponding energy spectrum. Pixels AB (3,4) at θ_{scatt} = 60°-65° (marked with "a" in the green area shown at Fig. 3 top panel), AB (8, -1) at θ_{scatt} = 80°-85° (marked with "c" in the pink area) and CD (-4, -3) at θ_{scatt} = 115°-120° (marked with "a" in the green area shown on Fig. 3, lower panel) are limiting cases just at the boundary of the region of T_{eff} > 3.5 um, where an overlap appears between the peaks of ^{10}C* and ^{208}Pb*.

The results of the simulations are summarised in Table 2, and the relevant spectra are shown in Fig. 4. The top panel displays the DE-Et spectrum for the pixel FG (5,5) at θ_{scatt} = 60°-65°, showing the locus of ^{10}C elastic (marked as $^{10}C_{el}$), inelastic (marked as ^{10}C*, ^{208}Pb*), and neutron transfer to ^{11}C (marked as $^{11}C_{tr}$). They are clearly separated in energy in the bidimensional plot, and the integration becomes straightforward in the *Et* projection shown in the left figure of the central panel (note the logarithmic scale in the vertical axe); the energy resolution (FWHM) is < 350 keV. The rest of the pictures show *Et* spectra for the pixels AB (3,4) at θ_{scatt} = 60°-65°, AB (8, -1) at θ_{scatt} = 80°-85° and CD (-4, -3) at θ_{scatt} = 115°-120°. Although there is some overlap between ^{10}C*(3.35 MeV) and ^{208}Pb*(2.6 MeV), the FWHM < 400 keV and the corresponding figure-of-merit FoM ~ 0.9 forecasts a good energy separation.

Also shown in Table 2 are the statistics expected for the selected angles, after adding the corresponding pixels, considering as requested 14 shifts (8 hours) of ^{10}C beam at 70 MeV, with an intensity of 3.5 10^4 pps on target. We expect a statistical uncertainty better than 1% for the elastic channel at θ~80° (Coulomb rainbow), better than 5% for the inelastic and neutron transfer channels ^{10}C* at θ ~ 115° and 80° (maximum) respectively.

Therefore, we conclude that our device can distinguish between both channels and disentangle the excitation of the Pb target from that of ^{10}C.

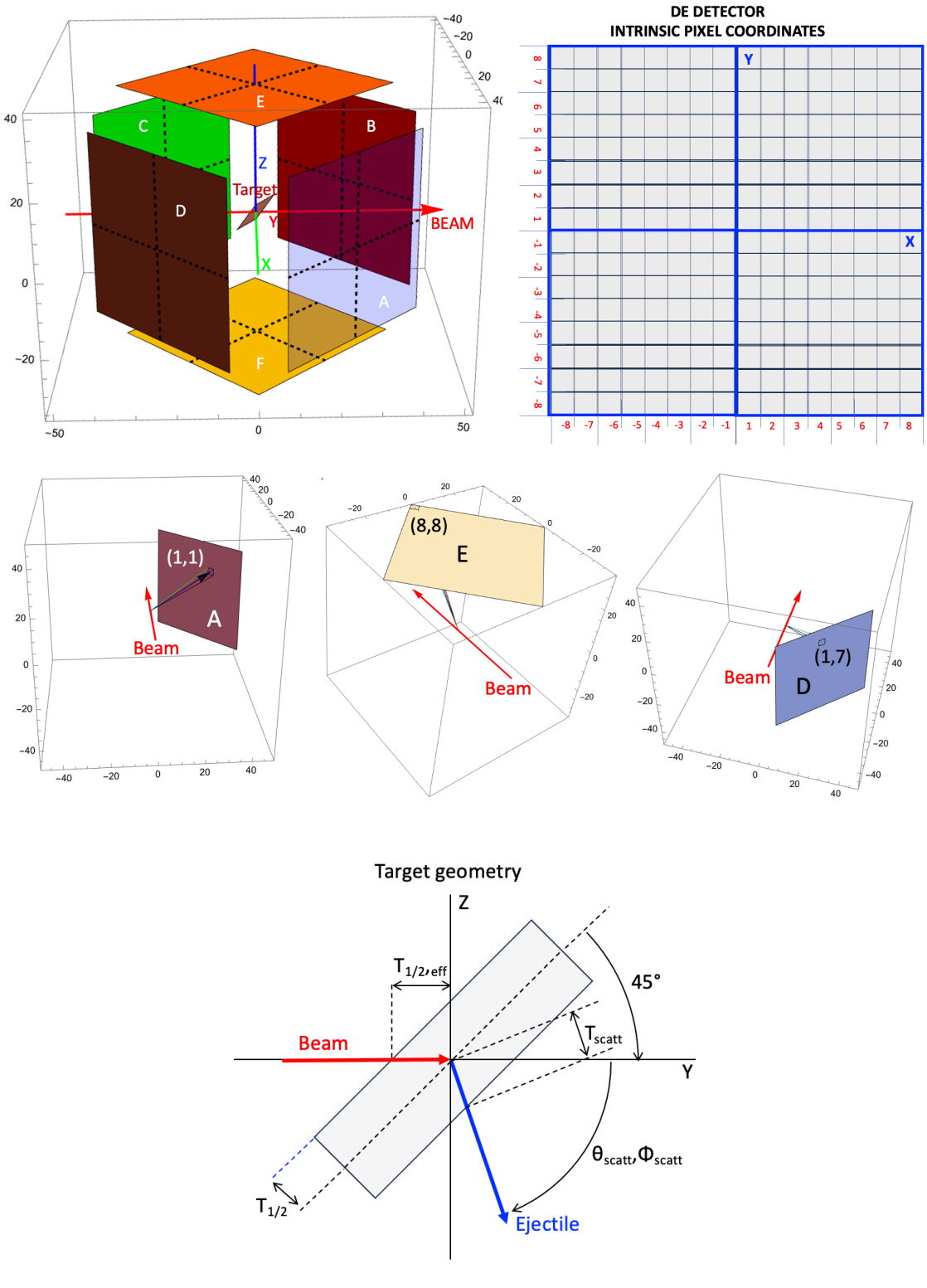

Figure 2. *Implementation of the GLORIA geometry in Mathematica. Upper panel: (left) complete system showing the forward detectors (A, B), upper/lower detectors (E, F) and backward detectors (C, D); (right) Intrinsic coordinates X, Y of detector pixels (in red). Central panel: a selection of pixels for detectors A (1,1), E (8,8) and D (1,7). Lower panel: Target geometry. See text for details.*

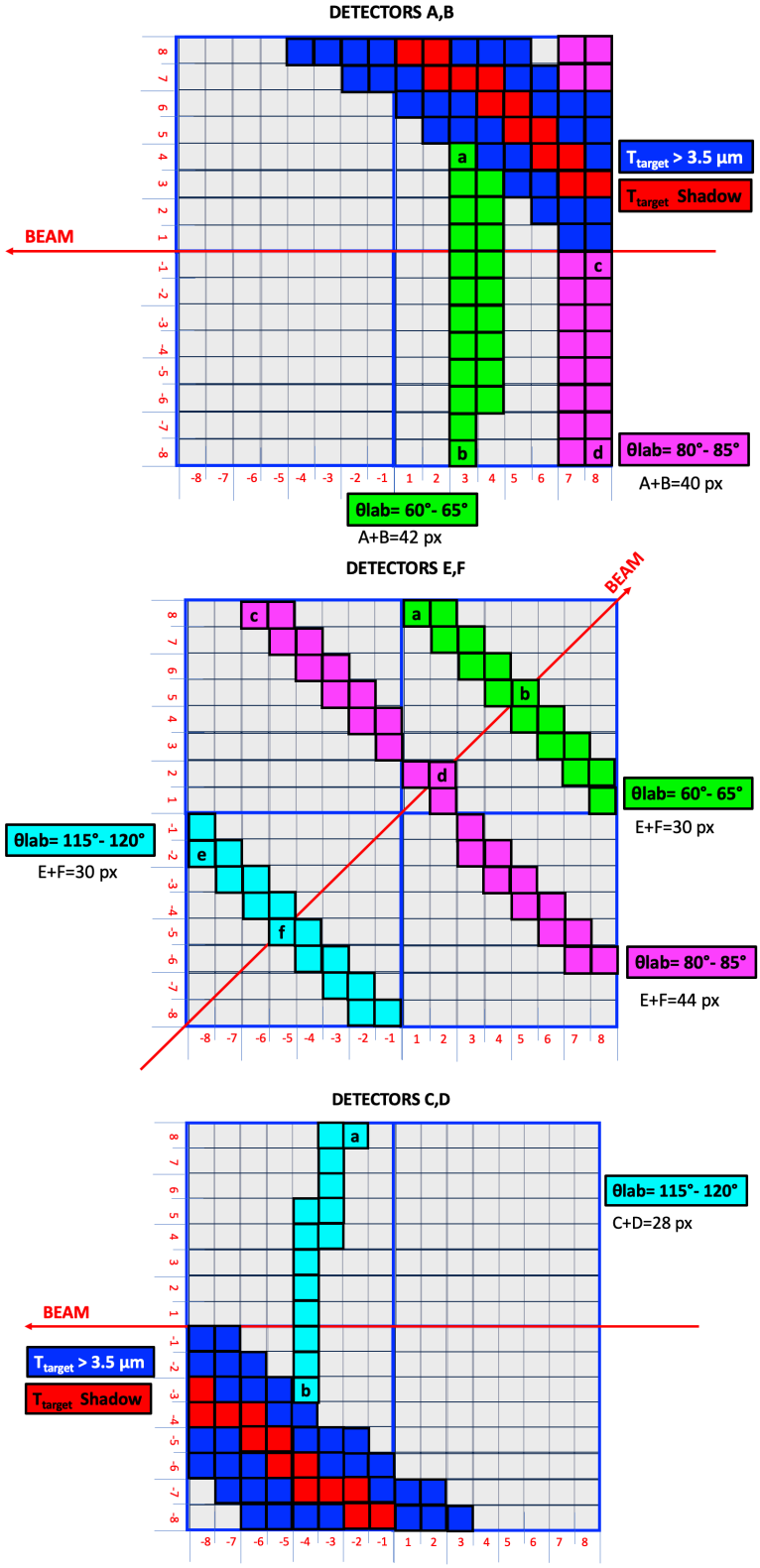

Figure 3. *Selected angular regions of the detector setup. Coloured regions correspond to pixels of 60°- 65° (green), 80°-85° (pink) and 115°-120° (light blue); the number of pixels used in the analysis is also shown. The pixels marked with dark blue correspond to angles in which the effective target thickness is more than 3.5 µm (red pixels correspond to the target shade ~ 90° lab scattering angle). Beam direction is indicated by a red arrow. See text for discussion.*

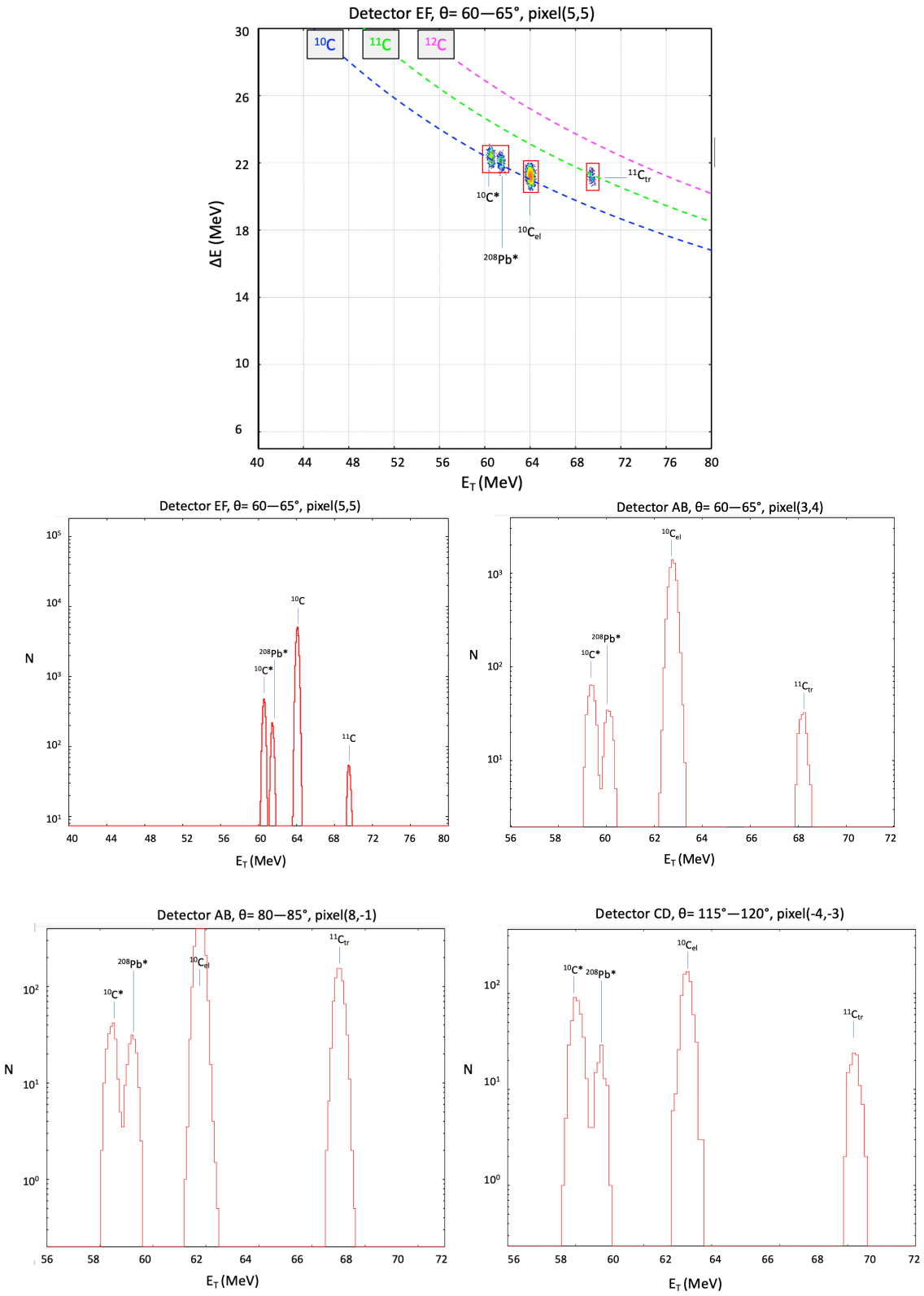

Figure 4. *Results of Montecarlo simulations for a selection of scattering angles and detector pixels. Top panel: DE vs Et plot of pixel (5,5) of detector EF, showing the locus of elastic Carbon-10 elastic events ($^{10}C_{el}$), inelastic Carbon-10 events from the excitation of Carbon-10 ($^{10}C^*$) and Lead-208 ($^{208}Pb^*$) and neutron transfer to ($^{11}C_{tr}$). The dashed lines corresponds to the locus of carbon masses 10 (blue dashes), 11(green dashes), 12 (pink dashes) using the approximation DE(Et)∝A/Et. Centre and lower panels show the Et projections for $^{10}C_{el,}$ $^{10}C^*$,$^{208}Pb^*$, and $^{11}C_{tr}$ for detector pixels: (5,5) of EF, (3,4) and (8,-1) of AB, (-4,-3) for CD. See text for discussion.*

		DETECTOR		
PIXEL (X,Y)		A,B	E,F	C,D
(-8,-8)	θ [°Lab]	30.99	134.44	99.76
	Ω [msr]	3.05	3.05	3.05
(-8,8)	θ [°Lab]	30.99	90.00	99.76
	Ω [msr]	3.05	3.05	3.05
(8,8)	θ [°Lab]	80.24	46.56	149.00
	Ω [msr]	3.05	3.05	3.05
(8,-8)	θ [°Lab]	80.24	90.00	149.00
	Ω [msr]	3.05	3.05	3.05
(1,1)	θ [°Lab]	47.61	86.39	137.49
	Ω [msr]	7.93	7.93	7.93

	PIXELS			TOTAL	SOLID ANGLE
ANGLE	A+B	E+F	C+D	PIXELS	[mb]
60-65	42	30	-	72	419.12
80-85	40	44	-	84	405.75
115-120	-	30	28	58	318.72

			Teff	ΔE
DETECTOR	ANGLE	PIXEL	[μm]	[μm]
A+B	60-65	(3,4)	3.52	42.85
E+F	60-65	(5,5)	2.14	46.00
A+B	80-85	(8,-1)	3.37	48.17
C+D	115-120	(-4,-3)	3.17	42.85

Table 1. *Summary of geometrical data for selected pixels of A, B, C, D, E, F detectors.*

			FWHM
DETECTOR	ANGLE	PIXEL	[keV]
A+B	60-65	(3,4)	369
E+F	60-65	(5,5)	331
A+B	80-85	(8,-1)	339
C+D	115-120	(-4,-3)	333

	σel(10C)	σin(10C)	σin(208Pb)	σtr(11C)
ANGLE	[mb/sr]	[mb/sr]	[mb/sr]	[mb/sr]
60-65	1044	8	4	2
80-85	458	8	4	20
115-120	26	20	4	4

	TOTAL EVENTS			
ANGLE	Elastic(10C)	Inelastic(10C)	Inelastic(208Pb)	Transfer(11C)
60-65	32939	253	126	63
80-85	13577	237	119	609
115-120	5721	437	87	96

Table 2. *Summary of the result of the Montecarlo simulations*

- ***Secondly, the elastic-scattering calculations shown in Fig. 4(a) of the proposal exhibit a Coulomb rainbow, whereas such a feature is not observed in the Texas A&M data, nor is it in the CDCC calculations performed to analyse them [see Fig. 7 of PRC 103, 044613 (2021)].***

As discussed in the proposal, the most recent experimental study of the $^{10}C+^{208}Pb$ scattering system at Coulomb barrier energies (Vb~ 60 MeV) was carried out by Linares et al. PRC 103, 044613 (2021) at *Texas A&M* at 66 MeV. The elastic-scattering calculation shown in Fig. 4(a) of our proposal exhibits a Coulomb rainbow since it is obtained from a CC calculation like the one performed by Linares et al., Fig. 6 which also exhibits a Coulomb rainbow, i.e., the authors of the *Texas A&M experiment* cannot reproduce their own data using the CC. To supress the rainbow and get closer to the data, Linares et al. introduced the coupling to the continuum process, in a similar manner to the description of neutron halo systems like ^{6}He or ^{11}Li, by means of a CDCC approach with 3- and 4-body models. But although the CDCC calculation solves the "Coulomb rainbow problem", the authors discover that the calculated angular distribution is not at all consistent with the measured data above 70 degrees (see e.g., Fig. 7, PRC 103, 044613 (2021)): the calculated distribution decreases too slowly between 70 - 100 degrees, and too fast between 100 - 140 degrees. Even more worrying, along the latter angular region the data show a large "bump", which is not at all described by the calculation. As a summary, the authors find that neither the CC nor the CDCC can describe the complete angular distribution. They justify the differences between theory and experiment as due to reaction processes related to the many-body structure of ^{10}C not considered in their calculations. Note that the excited state of $^{10}C^*$ is bound (on the contrary to ^{6}He or ^{11}Li), so it is not in the continuum, and thus not included in the CDCC.

However, the difficulties found by Linares et al. to describe their data are quite surprising, if we recall the good description achieved by Guimarães, et al. (PRC100, 034603 (2019)) using OM and CC for the elastic scattering data of system $^{10}C+^{58}Ni$ at 35.3 MeV measured at Notre Dame, also close to the Coulomb barrier (Vb~27 MeV). Furthermore, all the OM, CC and CDCC calculations of Guimarães et al., produce a Coulomb rainbow (Fig. 4, Fig. 10 of their paper). According to Guimarães, et al. coupling to $^{10}C^*$ inelastic plays the most important role in the dynamics of the $^{10}C + ^{58}Ni$ system at Coulomb barrier energies, that's why the CC works so well, and their CDCC calculation in fact reveals that the effect of coupling to the continuum is quite small (not surprising as the continuum states in ^{10}C are at quite high excitation energy).

Thus, the experimental data for $^{10}C+^{208}Pb$ of Linares et al. at *Texas A&M* cannot be easily understood, unless there is something special related to the ^{208}Pb target, which deserves further investigation. One should note that the "bump" observed in the angular distribution around 100-140 degrees is consistent with the maximum of the $^{10}C^*$ excitation channel predicted by our CC calculations, so perhaps the "elastic" data analysis suffered from this contamination. These experiments are difficult and suffer from the experimental limitations of the setup (energy, angular, and isobaric resolution, see Fig. 2 of the paper), also the presence of ^{10}B as a beam contaminant and the effect of the carbon backed target may lead to the presence of other non-elastic events in the integrated ^{10}C region.

Thus, to understand the dynamics of the $^{10}C+^{208}Pb$ system, before invoking exotic reaction mechanisms associated with the structure of ^{10}C, one must first provide clean and precise experimental data of the relevant reaction channels, e.g., elastic, $^{10}C^*$ inelastic and ^{11}C transfer channels for the present case. This is what we propose in our experiment at HIE-ISOLDE In the proposed experiment we will take advantage of the more intense ^{10}C beams provided at HIE-ISOLDE, a self-supporting ^{208}Pb target, and the high-efficiency GLORIA detector system.

- ***The beam energy considered here (70 MeV) is very close to that of the previous experiment (66 MeV). What explains that difference?***

The proposed scattering beam energy of 70 MeV is over the Coulomb barrier by about ~ 10 MeV (Vb~ 60 MeV Lab), and the experiment of Linares et al. was performed at 66 MeV Lab, about ~ 6 MeV above. This corresponds to the reaction points at ER=1.5 and ER=2 in Fig. 5 of Linares et al., respectively. The aim of the proposal is not to redo the *Linares et al.* experiment, but to provide

scattering data for the $^{10}C+^{208}Pb$ system which can serve to understand the reaction dynamics at energies around the Coulomb barrier. At the proposed 70 MeV beam energy the inelastic ($^{10}C^*$) and transfer cross sections (^{11}C) are larger than at 66 MeV, and the yield is enough to deliver the statistics required to study the coupling effects, considering the ^{10}C beam intensity available at HIE-ISOLDE, and a minimum request of shift numbers. Our theoretical estimates give for this energy a differential cross section of about ~10 - 20 mb for both $^{10}C^*$ inelastic and ^{11}C transfer between 60 - 140 deg. and 60-110 deg. respectively, the angular regions relevant for the physics case. Our collaboration has a large experience measuring elastic and reaction cross sections down to ~ 1 mb with the GLORIA array. On the other hand, and very important is the energy spread of the beam and reaction fragments induced by the 1 mg/cm^2 thick lead target, which is considerably smaller at 70 MeV than at 66 MeV Lab. This feature is relevant not only for separating the inelastic $^{10}C^*$ from the (weak) contribution of $^{208}Pb^*$, but also for improving the mass resolution of the DE-E particle telescopes. The choice of 70 MeV beam energy will thus increase cross sections and improve the overall response of the detector system, while keeping the reaction dynamics close to the Coulomb barrier.

- ***What are the channels that are included in the proponents' calculations?***

The calculations included inelastic excitation of the 3.35 MeV ^{10}C 2+ and 2.64 MeV, 3.20 MeV and 4.09 MeV ^{208}Pb 3-, 5- and 2+ levels, plus neutron pickup populating six levels of ^{207}Pb up to an excitation energy of 3.41 MeV and proton stripping to six levels of ^{209}Bi up to an excitation energy of 3.64 MeV.

- ***Can they reproduce the calculations shown in the Texas A&M paper? ^{10}C exhibits a very complicated structure because ^{9}C is proton unbound, and ^{8}Be, which is suggested as the core of the nucleus, is particle unbound too (it decays into two alphas). Can this reaction be understood within a simple two- or even three-body model of the nucleus? As advocated by Linares et al., doesn't this require a four-body model of ^{10}C (two alphas and two protons)?***

The elastic-scattering calculation shown in **Fig. 4(a) of the IS-666 proposal** is obtained from a CRC calculation similar to the CC one performed by Linares et al. shown in **Fig. 6 of R. Linares et al., PRC 103, 044613 (2021)** *(*see *Section: Relevant Figures* below*).* Both calculations give similar results, including the large Coulomb rainbow which lies completely out of the data. To supress the Coulomb rainbow and get closer to the "elastic" data, Linares et al. introduce the coupling to the continuum by means of a CDCC calculation but cannot describe the "bump" observed between 100-140 degrees. We didn't present CDCC calculations in our proposal, so we do not show the removal of the Coulomb rainbow due to continuum couplings as is done in the paper of Linares et al. The CDCC is a very time-consuming calculation, and it will not add any relevant information for planning the experiment; we believe it is not necessary before having the experimental data. As discussed by V. Guimarães, et al. PRC100, 034603 (2019), Fig. 4 and Fig. 10 (see *Section: Relevant Figures* below), in the case of the $^{10}C + ^{58}Ni$ system at Coulomb barrier energies, the coupling to the continuum is not so relevant, $^{10}C^*$ excitation and reorientation being the most important processes. The reduced coupling to the continuum compared to neutron haloes can be understood from the rather high energy of the continuum states associated with the possible cluster configurations. We agree with the referees in that a realistic calculation would need to consider the five body $^{10}C \rightarrow p+p+\alpha+\alpha$ configuration, which is still quite a challenge for theorists, and we expect to trigger these developments by providing good new data. However, V. Guimarães, et al. PRC100, 034603 (2019) achieved a satisfactory description of the data using CC and CDCC calculations. In any case, the reaction dynamics of the $^{10}C+^{208}Pb@70$ MeV is expected to be dominated by $^{10}C^*$ excitation and, eventually, the transfer to ^{11}C and ^{9}B.

Summarising, the dynamics of ^{10}C at Coulomb barrier energies is still an important puzzle to be solved.

Section: Relevant Figures

- *R. Linares et al., PRC 103, 044613 (2021)*

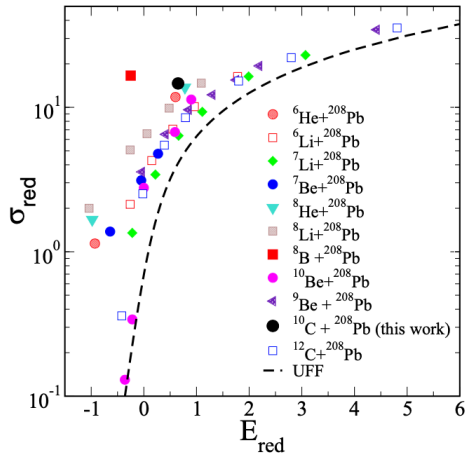

FIG. 5. Reduced reaction cross section for the several projectiles on ^{208}Pb target. The universal fusion function (UFF) is also shown in the plot as a lower bound to the reduced reaction cross sections.

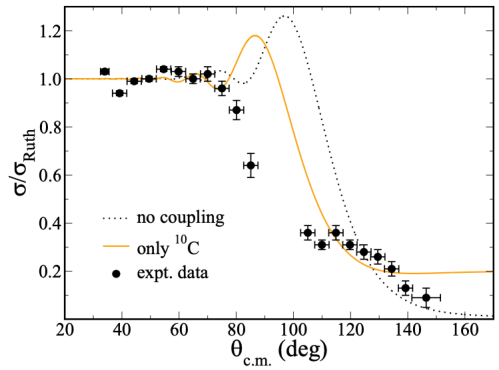

FIG. 6. Comparison between data and coupled-channels calculations for the elastic angular distribution for the ^{10}C + ^{208}Pb system at $E_{lab} = 66$ MeV. The no-coupling and the coupled-channel calculations are represented by dotted black and solid orange curves, respectively.

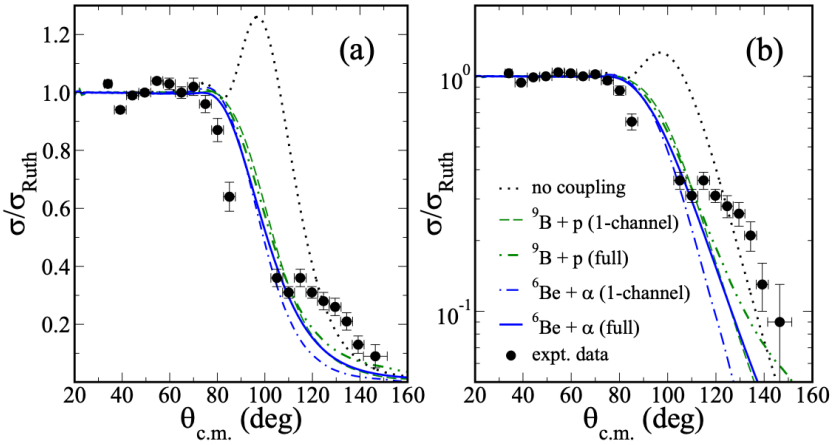

FIG. 7. Comparison between data and 3b-CDCC calculations considering the ^{9}B + p (green curves) and ^{6}Be +α (blue curves) cluster configurations in (a) linear scale and (b) log scale. The no-coupling calculation, presented in the previous subsection, is also included (dotted black curve). See text for details.

- *V. Guimarães, et al. (PRC100, 034603 (2019)*

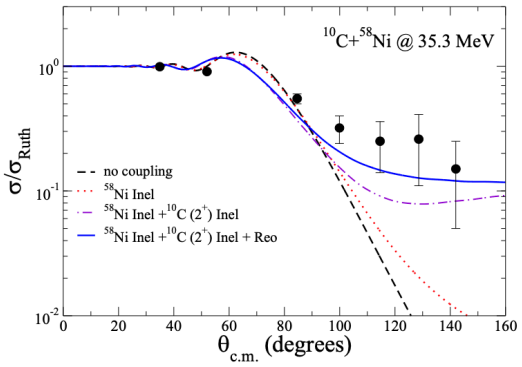

FIG. 4. Elastic scattering angular distribution for the ^{10}C + ^{58}Ni system at $E_{Lab} = 35.3$ MeV. The curves are the results of coupled-channels calculations as indicated. "Reo" implies inclusion of reorientation effects.

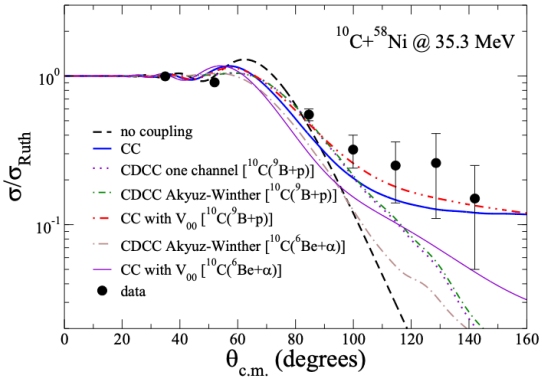

FIG. 10. Elastic-scattering angular distribution for the ^{10}C + ^{58}Ni system at $E_{Lab} = 35.3$ MeV. The curves are the results of CC and CDCC calculations.

ANNEX 1. INTC report

INTC-P-666 Study of the Coulomb barrier scattering of ^{10}C with heavy targets (15 shifts requested)

The aim of this proposal is to measure the scattering of ^{10}C from Pb at 70 MeV. In particular, it is suggested that the experimental setup will enable the separate measurements of the elastic, inelastic and one-neutron pickup channels. This renewed interest in the measurement of the scattering of exotic nuclei has been triggered by the measurement performed by Di Pietro et al. with ^{9,10,11}Be on Zn around the Coulomb barrier [Di Pietro *et al.* Phys Rev. Lett. **105**, 022701 (2010)]. While the elastic-scattering cross section for ^{10}Be is very similar to that for the stable ^{9}Be, the cross section for ^{11}Be, a well-known one-neutron halo nucleus, does not exhibit the usual Coulomb rainbow. Analyses within precise reaction models have shown that this was due to a significant coupling towards the breakup channel, in which the halo neutron dissociates from the core due to the interaction with the target. Similar effects have also been observed for the elastic scattering of two-neutron halo nuclei ^{6}He and ^{11}Li.

This kind of study has been later extended to the proton-rich side of the valley of stability. For the candidate one-proton halo nucleus ^{8}B, no such reduction of the Coulomb rainbow has been observed, although the breakup of this nucleus is also significant. However, it has been seen for ^{17}Ne, a probable two-proton halo nucleus. To understand this difference, further studies have been performed close to the proton dripline. In 2014, the elastic-scattering of ^{10}C on Pb has been measured at 226 and 256 MeV in Lanzhou [Yang *et al.* PRC **90**, 014606 (2014)]. As expected for this rather deeply bound nucleus – its S_{2p}=3.8 MeV– the authors observe a clear Coulomb rainbow for that system. More recently an experiment has been performed at Texas A&M to measure the elastic scattering of ^{10}C on Pb at 66MeV, i.e. close to the Coulomb barrier. Interestingly a reduction of the Coulomb rainbow was observed [Linares *et al.*, PRC **103**, 044613 (2021)]. Coupled-channel calculations with a discretised continuum (CDCC) could reproduce most of the features of the experimental cross section, including the absence of the Coulomb rainbow. Unfortunately, some features of the data could not be properly explained by the CDCC calculations, in particular a peak at backward angles. One possible reason for this issue is that the experiment could not disentangle between elastic and inelastic scattering. A new, more precise measurement of the elastic scattering of ^{10}C on Pb around the Coulomb barrier, especially one that can distinguish the elastic and inelastic channels, might help us understand this discrepancy between theory and experiment. This is the goal of proposal P-666.

However, the proposal does not include any realistic simulation of the planned measurement. Prior to acceptance it is important to make sure that the detection device can disentangle between the elastic and inelastic channels. The proponents should prove that their devices can distinguish between both channels. They should also say whether they can disentangle the excitation of the Pb target from that of ^{10}C.

Secondly, the elastic-scattering calculations shown in Fig. 4(a) of the proposal exhibit a Coulomb rainbow, whereas such a feature is not observed in the Texas A&M data, nor is it in the CDCC calculations performed to analyse them [see Fig. 7 of PRC **103**, 044613 (2021)]. The beam energy considered here (70MeV) is very close to that of the previous experiment (66MeV). What explains that difference? What are the channels that are included in the proponents' calculations? Can they reproduce the calculations shown in the Texas A&M paper? ^{10}C exhibits a very complicated structure because ^{9}C is proton unbound, and ^{8}Be, which is suggested as the core of the nucleus, is particle unbound too (it decays into two alphas). Can this reaction be understood within a simple two- or even three-body model of the nucleus? As advocated by Linares *et al.*, doesn't this require a four-body model of ^{10}C (two alphas and two protons)?

To better understand both the interest and feasibility of this experiment, the INTC requests a clarification letter that provides an answer to these different issues.